International Journal of Nanomedicine

Dovepress
open access to scientific and medical research

Open Access Full Text Article

ORIGINAL RESEARCH

Core–shell magnetic nanoparticles display synergistic antibacterial effects against *Pseudomonas aeruginosa* and *Staphylococcus aureus* when combined with cathelicidin LL-37 or selected ceragenins

This article was published in the following Dove Press journal:
International Journal of Nanomedicine
19 October 2016
Number of times this article has been viewed

Katarzyna Niemirowicz[1] Ewelina Piktel,[1] Agnieszka Z Wilczewska,[2] Karolina H Markiewicz,[2] Bonita Durnaś,[3] Marzena Wątek,[4] Irena Puszkarz,[3] Marta Wróblewska,[5,6] Wiesława Niklińska,[7] Paul B Savage,[8] Robert Bucki[1,3]

[1]Department of Microbiological and Nanobiomedical Engineering, Medical University of Białystok, [2]Institute of Chemistry, University of Białystok, Białystok, [3]Department of Physiology, Pathophysiology and Immunology of Infections, The Faculty of Health Sciences of the Jan Kochanowski University in Kielce, [4]Holy Cross Oncology Center of Kielce, Kielce, [5]Department of Dental Microbiology, Medical University of Warsaw, [6]Department of Microbiology, Central Clinical Hospital in Warsaw, Warsaw, [7]Department of Histology and Embryology, Medical University of Bialystok, Białystok, Poland; [8]Department of Chemistry and Biochemistry, Brigham Young University, Provo, UT, USA

Correspondence: Robert Bucki
Department of Microbiological and Nanobiomedical Engineering, Medical University of Białystok, Mickiewicza 2 C, 15-222 Białystok, Poland
Tel +48 85 748 5483
Fax +48 85 748 5492
Email buckirobert@gmail.com

Abstract: Core–shell magnetic nanoparticles (MNPs) are promising candidates in the development of new treatment methods against infections, including those caused by antibiotic-resistant pathogens. In this study, the bactericidal activity of human antibacterial peptide cathelicidin LL-37, synthetic ceragenins CSA-13 and CSA-131, and classical antibiotics vancomycin and colistin, against methicillin-resistant *Staphylococcus aureus* Xen 30 and *Pseudomonas aeruginosa* Xen 5, was assessed alone and in combination with core–shell MNPs. Fractional inhibitory concentration index and fractional bactericidal concentration index were determined by microdilution methods. The potential of combined therapy using nanomaterials and selected antibiotics was confirmed using chemiluminescence measurements. Additionally, the ability of tested agents to prevent bacterial biofilm formation was evaluated using crystal violet staining. In most conditions, synergistic or additive effects were observed when combinations of core–shell MNPs with ceragenins or classical antibiotics were used. Our study revealed that a mixture of membrane-active agents such as LL-37 peptide or ceragenin CSA-13 with MNPs potentialized their antibacterial properties and might be considered as a method of delaying and overcoming bacterial drug resistance.

Keywords: synergistic activity, antibiotic-resistant bacteria, LL-37 peptide, ceragenins, magnetic nanoparticles

Introduction

The overuse and misuse of antibiotics have led to the emergence of bacterial resistance, which has become a key problem in modern medicine.[1] Reduced susceptibility of bacteria to antibiotics is particularly an important issue during treatment of infections in hospitalized patients. Many of resistant strains cause infections in intensive care and hemato-oncology units. Indeed, increased cost of these patients' treatment has motivated the search for new methods of prevention and therapy.[2,3]

Leading nosocomial pathogens, such as methicillin-resistant *Staphylococcus aureus* (MRSA) and multidrug resistant (MDR) *Pseudomonas aeruginosa*, are difficult to eradicate due to their resistance to many antibiotics introduced over the last few decades. *S. aureus* is a widespread human commensal causing skin, soft tissue, and bone infections.[4] It can also be responsible for pneumonia and sepsis. For most MRSA strains, antibiotics from the glycopeptide family are the only therapeutic option.[5–7]

submit your manuscript | www.dovepress.com
Dovepress
http://dx.doi.org/10.2147/IJN.S113706

Infections with *P. aeruginosa* are of concern particularly for people with severe burns and immunocompromised patients and adults with cystic fibrosis.[8,9] Moreover, *S. aureus* and *P. aeruginosa* possess the ability to form biofilms that facilitate the colonization of medical devices, thereby contributing to the spread of drug-resistant strains in a hospital environment.[10,11]

Improvement of the bactericidal action of currently used antibiotics, by expanding their spectrum of activity, might be achieved using a strategy offered by nanotechnology in conjunction with nontraditional antibiotic agents such as synthetic cationic lipids, which have great potential in overcoming pathogen resistance.[12] Multiple recent studies have focused on the use of core–shell magnetic nanoparticles (MNPs), which show unique biological and physicochemical properties. They are widely used in biomedicine as diagnostic tools or drug delivery systems in personal therapy.[13–16] Our recent studies indicate that core–shell MNPs might act as antimicrobial agents via destruction of bacterial cell membrane and interaction with surface proteins.[17,18] Furthermore, it has been reported that nanoparticles penetrate biofilms, destroy spore-forming bacteria, and are active against MDR pathogens.[17,19,20] The enhancement of the efficiency of antimicrobial agents due to their covalent or electrostatic immobilization on the surface of the nanoparticles and co-treatment using nanomaterials containing combinations is a preferable approach in the treatment of bacterial and fungal infections.[21–23] The mixed therapy constitutes a method to increase the effectiveness of antibiotic treatment with subsequent reduction in its doses and potential adverse effects. To date, it was demonstrated that silver nanoparticles possess the great potential to be used in the treatment of MDR bacteria, when combined with imipenem, gentamycin, vancomycin (VAN), ciprofloxacin, kanamycin, and chloramphenicol.[24–26] Addition of silver nanoparticles enhances as well the antimicrobial and antibiofilm efficiency of ampicillin and VAN against both Gram-positive and Gram-negative bacteria due to increased reactive oxygen species generation.[27] Li et al[21] demonstrated that silver nanoparticles might be employed as an adjuvant compound in combination with cefmetazole against antibiotic-resistant *Neisseria gonorrhoeae*. However, only few studies have reported that the efficacy of antimicrobial agents can be improved when applied in combination with metallic nanoparticles.[23] Additionally, a limited number of them present this effect when combined with mimics of natural antimicrobial peptides.

In this study, we describe the antibacterial properties of different core–shell MNPs in combination with selected membrane-active agents such as cathelicidin LL-37 and ceragenins cationic steroid antibiotics (CSA)-13 and CSA-131 as well as with the classical antibiotics VAN and colistin (COL). Antibacterial activity was measured against Gram-positive MRSA Xen 30 and Gram-negative *P. aeruginosa* Xen 5 strains. We demonstrate that co-treatment with tested antibacterial agents in combination with MNPs is more effective than treatment with tested agents alone against planktonic or bacterial cells embedded in biofilm. Our results point toward a possibility of developing new strategies to treat infections caused by resistant pathogens by exploring synergy between antibacterial agents and their nanocarriers.

Materials and methods

Synthesis of core–shell MNPs

Iron oxide MNPs were synthesized by modification of Massart's method.[28] Gold (MNP@Au) and aminosilane (MNP@NH_2) coated MNPs were synthesized according to a previously published procedure with some modification.[17] Briefly, uncoated nanoparticles (0.6 g) were suspended in deionized water (20 mL), and NaOH (45 mmol), $HAuCl_4$ (7.85 mmol), $NaBH_4$ (6.6 mmol), and citric acid (20 mmol) were added and sonicated for 1 hour under argon gas protection. Next, the nanoparticles were washed three times with water and ethanol. Aminosilane shells were obtained by one-step polycondensation of 3-aminopropyltrimethoxysilane. Polymeric shells around gold-coated MNPs were created via modification of reversible addition-fragmentation chain transfer polymerization/macromolecular design by interchange of xanthates (RAFT/MADIX) polymerization of 4-chloromethylstyrene and its quaternary ammonium salt derivatives (MNP@PQAS – poly(quaternary ammonium salts)).[29] The quaternary ammonium salt styrene derivatives were obtained in situ via substitution reaction of 4-chloromethylstyrene with excess of amine (triethylamine) during the polymerization process. After 2 hours sonication at 60°C, nanoparticles were separated under a magnetic field and washed three times by toluene, methanol, and water. All nanoparticle samples, after the synthesis process, were dried to powder at 50°C for 12 hours.

Characterization of core–shell MNPs

To confirm the chemical structure and morphology of the fabricated nanoparticles, multiple techniques were used. Fourier transform infrared spectra were recorded in the wavenumber range of 4,000–500 cm^{-1} by co-adding 32 scans with a resolution of 4 cm^{-1}. Differential scanning calorimetry (DSC) was recorded on a Mettler Toledo Star DSC1 system. Nitrogen was used as a purge gas with a flow of 20 $mL \cdot min^{-1}$.

Nanoparticles (5 mg) were placed in aluminum pans and heated from 30°C to 450°C with a heating rate of 20°C/min. Thermogravimetric analysis (TGA) was performed using a Mettler Toledo Star TGA/DSC unit. Dry nanoparticles (2 mg) were placed in the aluminum pans (40 µL) and heated from 50°C to 800°C with a heating rate of 10°C/min. Transmission electron microscopy/energy-dispersive X-ray spectroscopy (Tecnai G2 X-TWIN) was used to characterize morphological features of synthetized MNPs.

Antimicrobial testing

To determine the minimum inhibitory concentration (MIC) of antimicrobial agents alone (LL-37, CSA-13, CSA-131, VAN, and COL) or their combinations with tested core–shell MNPs against *S. aureus* Xen 30 (a clinical MRSA isolate) and *P. aeruginosa* Xen 5 (human septicemia isolate; both possess a stable copy of the *Photorhabdus luminescens* lux operon on the bacterial chromosome; PerkinElmer Inc., Waltham, MA, USA), a serial microdilution method was performed using 96-well microtiter plates. Two-fold serial dilutions of MNPs and antimicrobial agents ranging from 256 µg/mL to 0.25 µg/mL were tested. The inoculum was adjusted to a final concentration of 1×10^5 CFU/mL by measuring the turbidity using a spectrophotometer (λ=600 nm). Plates containing the mixture of bacteria with antibiotics were incubated at 37°C for 24 hours. Following the incubation period, they were evaluated visually for the presence of bacterial growth. The lowest concentration of antimicrobial agent inhibiting bacterial growth was identified as the MIC value. Minimal bactericidal concentration (MBC) was determined by plating 10 µL of bacterial suspension containing a mixture of both antimicrobial agent and bacteria on Luria–Bertani agar plates, from the well matching the MIC values, followed by overnight incubation. A similar procedure for two prior wells containing correspondingly higher concentrations of the antibiotic was tested. Plates were assessed for bacterial growth. The lowest concentration indicating lack of growth was identified as the MBC.

Measurement of chemiluminescence intensity was performed as an additional method to evaluate antibacterial activity of LL-37 peptide, ceragenins CSA-13 and CSA-131, VAN, and COL alone and in combination with MNPs. Chemiluminescence intensity of *S. aureus* Xen 30 and *P. aeruginosa* Xen 5 was evaluated using Labsystem Varioscan Lux (Thermo Fisher Scientific, Waltham, MA, USA). Bacteria were grown to mid-log phase at 37°C, resuspended in Luria–Bertani broth, and brought to 10^9 CFU/mL. Then, 100 µL of bacteria suspension was added to each well containing 100 µg/mL of MNP@NH_2, MNP@Au, MNP@PQAS, LL-37, CSA-13, CSA-131, COL, VAN, or their combinations.

FIC/FBC determinations

To evaluate the interaction effects between core–shell MNPs, ceragenins, and classical antibiotics, fractional inhibitory concentration (FIC) index and fractional bactericidal concentration (FBC) index were determined. A mutual antimicrobial effect of the analyzed compounds was calculated as follows: FIC = MIC (A in combination with B)/MIC (A alone) + MIC (B in combination with A)/MIC (B alone), where A is defined as nanoparticles (MNP@NH_2, MNP@Au, or MNP@PQAS) and B as one of the tested agents. The same procedure was used to define the FBC, but for the calculation, MBC values were used. FIC/FBC values >4 indicate antagonistic effects, values between 4 and 1.01 indicate indifference, values between 1 and 0.76 indicate additive effects, and values <0.76–0.5 indicate partial synergy and <0.5 indicate synergistic effects.[30]

Antibiofilm activity

To determine the ability of core–shell MNPs to prevent biofilm formation, an incubation of *S. aureus* Xen 30 and *P. aeruginosa* Xen 5 with different concentrations (10 µg/mL, 50 µg/mL, and 100 µg/mL) of tested compounds was performed for 48 hours at 37°C. In each experiment, an overnight culture of pathogens was diluted to ~10^5 CFU/mL. Bacterial suspensions and analyzed agents were placed in 96-well polystyrene plates, and a biofilm was allowed to grow. After incubation, the medium was removed, and the wells were washed in order to remove planktonic cells. Biofilm was stained using 0.1% (w/v) crystal violet. After 15 minutes, crystal violet was removed, and the plates were thoroughly rinsed. In order to determine the mass of biofilm, crystal violet was solubilized in 95% ethanol. The amount of extracted stain corresponding to biofilm mass was assessed spectrophotometrically (λ=580 nm). Chemiluminescence intensities of *S. aureus* Xen 30 and *P. aeruginosa* Xen 5 cells embedded within a biofilm were evaluated as an additional determinant of biofilm viability. Chemiluminescence was measured using Labsystems Varioscan Lux (Thermo Fisher Scientific) and analyzed using SkanIt Software (data not shown).

Results

Nanoparticle characterization

The chemical structures of antimicrobial agents and core–shell MNPs are shown in Figure 1A. The iron oxide

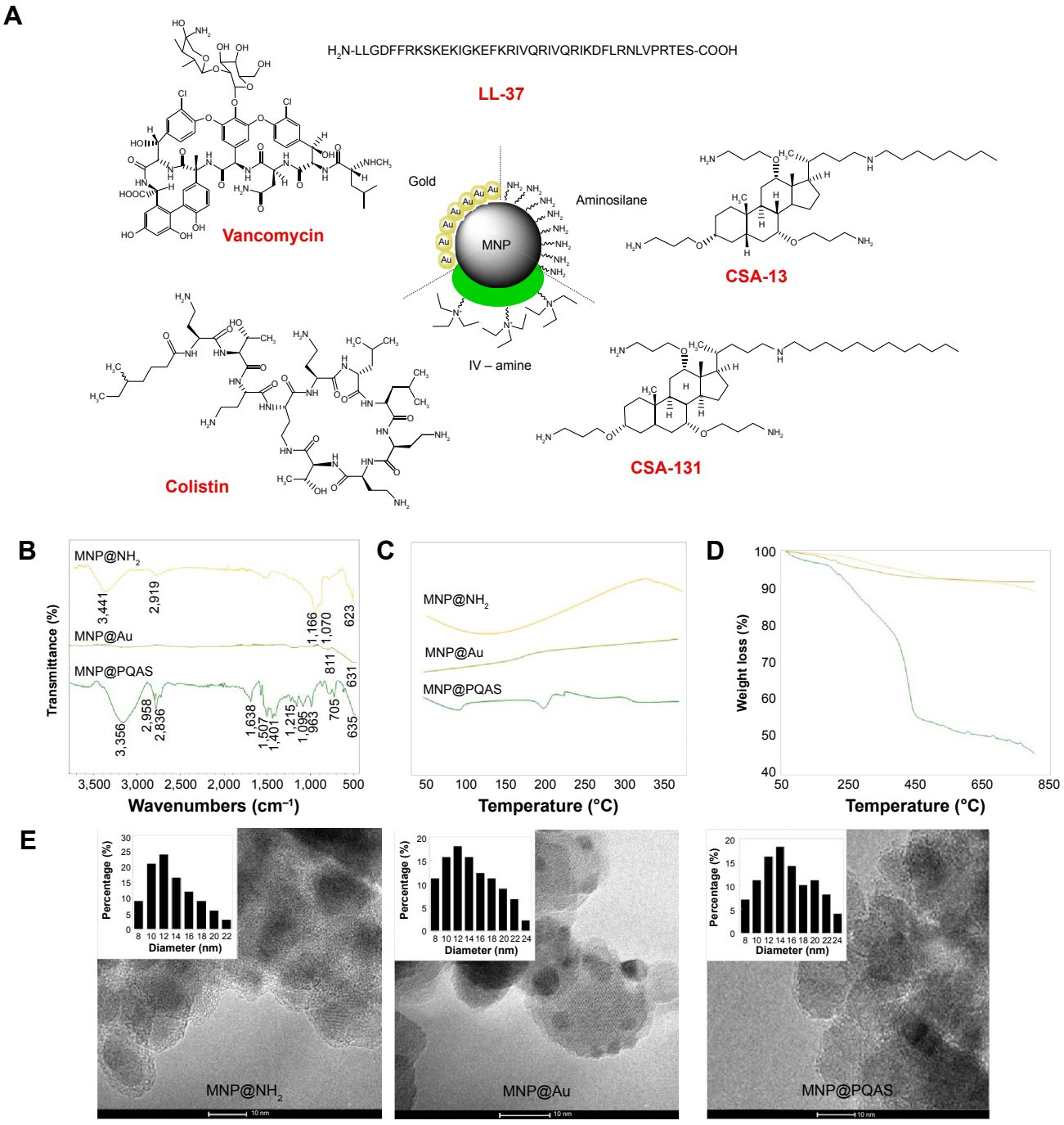

Figure 1 Structure and physicochemical properties of core–shell MNPs and antibacterial agents.

Notes: Schematic representation of core–shell nanostructure and chemical structure of tested antimicrobial agents (**A**). ATR FT-IR spectra of the aminosilane- (MNP@NH_2), gold- (MNP@Au), and PQAS-coated (MNP@PQAS) MNPs (**B**). (**C**) DSC analysis and (**D**) TGA curves. (**E**) Transmission electron microscopy images of aminosilane-, gold-, and PQAS-coated core–shell MNPs. Small images inside TEM images display particles' size distribution.

Abbreviations: MNP, magnetic nanoparticle; ATR, attenuated total reflectance; FT-IR, Fourier transform infrared; PQAS, poly(quaternary ammonium salts); DSC, differential scanning calorimetry; TGA, thermogravimetric analysis; TEM, transmission electron microscopy; LL-37, cathelicidine LL-37; CSA, cationic steroid antibiotic.

magnetic core was obtained according to the modification of Massart's method.[28] Subsequently, bare MNPs were treated with 3-aminopropyltrimethoxysilane to place an amino-terminated silica on their surface. Gold-coated nanoparticles were obtained via modification of the K-gold method.[31] Gold nanoparticles modified with dithiocarbonate (polymer chain transfer agent) were obtained by sonication of MNP@Au in toluene in the presence of symmetric dithiocarbonate (1:1, w/w). The suspension was sonicated for 24 hours in room temperature, then the precipitate was separated from solvent by using an external magnetic field, decanted, and rinsed with ethanol several times to remove the nonchemisorbed

dithiocarbonate. A RAFT/MADIX polymerization process was employed to cover the surface of gold-coated MNPs with a poly(methylstyrene quaternary ammonium salt) shell. Figure 1B shows attenuated total reflectance Fourier transform infrared spectra of aminosilane-, gold-, and PQAS-coated MNPs (MNP@NH_2, MNP@Au, MNP@PQAS), respectively. The existence of an iron oxide magnetic core in all samples is indicated by a band around 623–635 cm^{-1}, which corresponds to the Fe–O stretching mode of magnetite (Fe_3O_4). The spectrum of aminosilane-coated nanoparticles shows a broad band at ~1,066–1,170 cm^{-1} associated with the stretching vibrations characterized for organosilane derivatives including Si–O, Si–O–Si, and Si–O–Fe. The band above 3,400 cm^{-1} corresponds to N–H stretching vibrations. The adsorption signal at 811 cm^{-1} was detected at the spectrum of gold-coated MNPs. After functionalization of MNP@Au with a PQAS shell, a signal at 1,215 cm^{-1} was detected and ascribed to C–N stretching vibrations. The bands observed in the area of 2,836–2,958 cm^{-1} were assigned to stretching vibrations of C–H from alkyl groups, while the signals >3,000 cm^{-1} were attributed to stretching vibrations of C–H from aromatic groups. In addition, the bands from 1,638 cm^{-1} to 1,401 cm^{-1} were identified as a C–C stretching mode of an aromatic ring. Signals observed at 1,095 cm^{-1} and 705 cm^{-1} correspond to the bending vibrations of C–H bonds in and out of plane (C-Hoop). The thermal properties of core–shell nanostructures were characterized by DSC (Figure 1C). The heating curves of aminosilane-, gold-, and quaternary ammonium salt derivative-coated MNPs indicate differences in the chemical nature of coating. Figure 1D shows the TGA of the three above-mentioned MNPs. It was previously noted that bare iron oxide MNPs show 6% weight loss in the temperature range of 50°C–800°C, which is directly associated with the loss of adsorbed water and decomposition of hydroxyl surface groups.[32] The TGA curves show that the weight loss of aminosilane- and gold-coated MNPs during the performed analysis was close to 7% and 4%, respectively. The TGA of nanoparticles coated by PQAS showed a total weight loss of 55%. The 45% weight loss of the MNP@PQAS (compared to the weight loss of bare and MNP@Au) indicates a successful coating by RAFT/MADIX polymerization. The transmission electron microscopy-based techniques were used to evaluate the size and the morphology of the core–shell nanoparticles. The particles were found to be spherical, and an average size was estimated as 12 nm, 11 nm, and 13 nm for aminosilane-, gold-, and quaternary ammonium derivative-coated MNPs, respectively (Figure 1E). This result was also confirmed by X-ray diffraction technique (Williamson–Hall method).[33]

The combination of antibacterial agents with MNPs increases their bactericidal effect

One of the widespread and most accepted methods to assess bactericidal properties of antimicrobial compounds against the planktonic form of bacteria is determination of MIC and MBC values. As presented in Table 1, ceragenins CSA-13 and CSA-131 exert high antimicrobial effect and possess the potential for application as novel antibacterial agents in the treatment of bacterial infections, especially those caused by Gram-positive bacteria, since its activity is higher against *S. aureus* than *P. aeruginosa*. Importantly, both ceragenins act stronger when compared to LL-37 peptide, and their activity is comparable with activity of COL and VAN.

Additionally, assessment of MIC/MBC values for samples co-treated with nanoparticles and selected antibiotics suggested that administration of combined treatment is more effective than therapy with antibacterial agents alone. Particularly, addition of MNPs reduces the MIC/MBCs values of ceragenins and conventional antibiotics up to fourfold. Combined treatment using MNPs allowed a reduction in the MIC of VAN against *S. aureus* to 1 μg/mL (originally 4 μg/mL) and gave a low CSA-13 concentration that eradicates *P. aeruginosa* Xen 5 (2 μg/mL; originally 8 μg/mL). However, the largest alternation in killing activity was shown for LL-37 in combination with gold-coated nanoparticles (MNP@Au + LL-37). The significant increase of antimicrobial activity was observed against both *P. aeruginosa* and *S. aureus* strains – it was assessed that doses of 2 μg/mL and 4 μg/mL of this combination were required to inhibit bacterial growth of tested bacterial strains, which demonstrates 64-fold and 32-fold

Table 1 MICs and MBCs of tested agents against *Staphylococcus aureus* Xen 30 and *Pseudomonas aeruginosa* Xen 5

Agents	MRSA Xen 30		*P. aeruginosa* Xen 5	
	MIC (μg/mL)	MBC (μg/mL)	MIC (μg/mL)	MBC (μg/mL)
LL-37	128	128	128	256
CSA-13	0.5	1	8	16
CSA-131	0.5	1	8	16
COL	ND	ND	1	2
VAN	4	8	ND	ND
MNP@NH_2	64	128	128	256
MNP@Au	64	128	16	64
MNP@PQAS	128	128	64	128

Abbreviations: MICs, minimal inhibitory concentrations; MBC, minimal bactericidal concentration; MRSA, methicillin-resistant *S. aureus*; LL-37, cathelicidine LL-37; CSA, cationic steroid antibiotic; COL, colistin; ND, not determined; VAN, vancomycin; MNP, magnetic nanoparticle; PQAS, poly(quaternary ammonium salts).

decrease in the original MIC value of LL-37 peptide (data not shown).

To establish the results obtained from MIC/MBC measurements, luminometric analysis of bacterial survival after treatment with tested agents was performed. Monitoring luminescence as a measure of metabolic activity provides a rapid determination of bacterial growth and viability.[34] First, antimicrobial potential of synthetized nanoparticles was confirmed. As presented in Figure 2A and B, all nanomaterials employed in our study strongly affect the viability of *S. aureus* and *P. aeruginosa* strains. Particularly, an 80% decrease of chemiluminescence was observed after treatment of both pathogens with gold-coated MNPs. In agreement with previous reports, it was also confirmed that ceragenins CSA-13 and CSA-131 strongly affect the metabolism and viability of tested bacterial strains, resulting in a 50% reduction of chemiluminescence intensity. In contrast, the decrease of light signal after treatment with classical antibiotics alone reached ~20%. Importantly, a significant decrease of chemiluminescence, up to 99%, was observed after the addition of MNPs. As indicated in Figure 2C–F, combination of VAN, CSA-13, CSA-131, or LL-37 with MNPs results in rapid reduction of luminescence intensity recorded from *S. aureus* Xen 30 culture. A similar effect was observed for *P. aeruginosa* Xen 5 culture, where an analysis of the impact of nanoparticles with COL, CSA-13, CSA-131, and LL-37 peptide was evaluated (Figure 2G–J). This decrease was several times lower compared to controls and bacteria cultures treated with antibacterial agents alone, which confirms the high potential of nanoparticles-containing combined treatment. It is also noteworthy that addition of nanomaterials does not alter the kinetics of antimicrobial killing, and the majority of bacteria are eradicated within first 2 minutes. Among all analyzed types of MNPs, we observed slight differences between the degrees of potentiation of ceragenins in antibacterial properties. However, from these observations, we conclude that gold-coated nanoparticles (MNP@Au) display the greatest potential for synergistic properties. For conventional antibiotics, VAN and COL, no significant differences were observed using various nanomaterials.

MNPs exhibit a synergistic or an additive effect in combination with LL-37, CSA-13, CSA-131, VAN, or COL

MIC and MBC values were used to calculate the FIC and FBC index, and results are shown in Tables 2 and 3 (FIC index) and Tables 4 and 5 (FBC index). These results indicate the existence of an additive effect between MNPs, LL-37 peptide, CSA-13, CSA-131, and tested conventional antibiotics. With some combinations, a synergistic or partially synergistic effect was observed. Notably, no antagonistic effects were observed in any of the analyzed combinations of bactericidal agents with MNPs. The analysis of obtained FIC/FBC index allows to perform an assessment, which combinations are the best for individual antimicrobial agents. According to the data presented in Tables 2–5, it is hypothesized that LL-37 exerts highest bactericidal effect when combined with gold-coated nanoparticles (MNP@Au). The potentiation of antimicrobial activity of CSA-13 depends on tested bacterial strain – CSA-13 eradicates MRSA Xen 30 most effective in combination with MNP@Au, but against *P. aeruginosa* Xen 5 the best combination is co-treatment with MNP@NH_2. Aminosilane-coated nanoparticles enhance as well the activity of CSA-131 against *P. aeruginosa* Xen 5. Synergistic effect was observed for the combination of VAN with MNP@PQAS. In contrast to that, it is assumed that improvement of bactericidal activity of COL does not depend on the properties of nanoparticles surface, since no significant differences were observed using different nanomaterials in combination with this antibiotic.

MNPs increase the ability of LL-37, CSA-13, and CSA-131 to prevent biofilm formation

The restriction of biofilm growth as the result of antibiotic therapy is a favorable approach in the treatment of infections. However, its eradication is considerably hampered due to variety of factors and compounds associated with its formation.[35] Figure 3A–D illustrates that antimicrobial agents alone are able to prevent biofilm formation by MRSA Xen 30 strain and effectively kill bacteria embedded into the biofilm matrix. Nevertheless, high doses (>50 μg/mL) are required to obtain inhibition of biofilm formation in the 40%–50% range. When combined with MNP@NH_2, treatment with antibacterial compounds (10 μg/mL) decreases biofilm formation by 40% for LL-37 (Figure 3A) and 60% for VAN (Figure 3D). A decrease of 85% in biofilm formation was measured with a combination of CSA-131 with MNP@PQAS (Figure 3C). Strong antibiofilm effect was noted as well for *P. aeruginosa* Xen 5 (Figure 3E–H). With the combination of COL with MNP@Au, a decrease of 70% in biofilm (Figure 3H) was recorded. Lack of adhesion of both tested bacterial strains to a polystyrene surface was noted at a concentration of 50 μg/mL for VAN in combination with MNP@Au and MNP@PQAS (Figure 3D) and for COL combined with all tested nanostructures (Figure 3H).

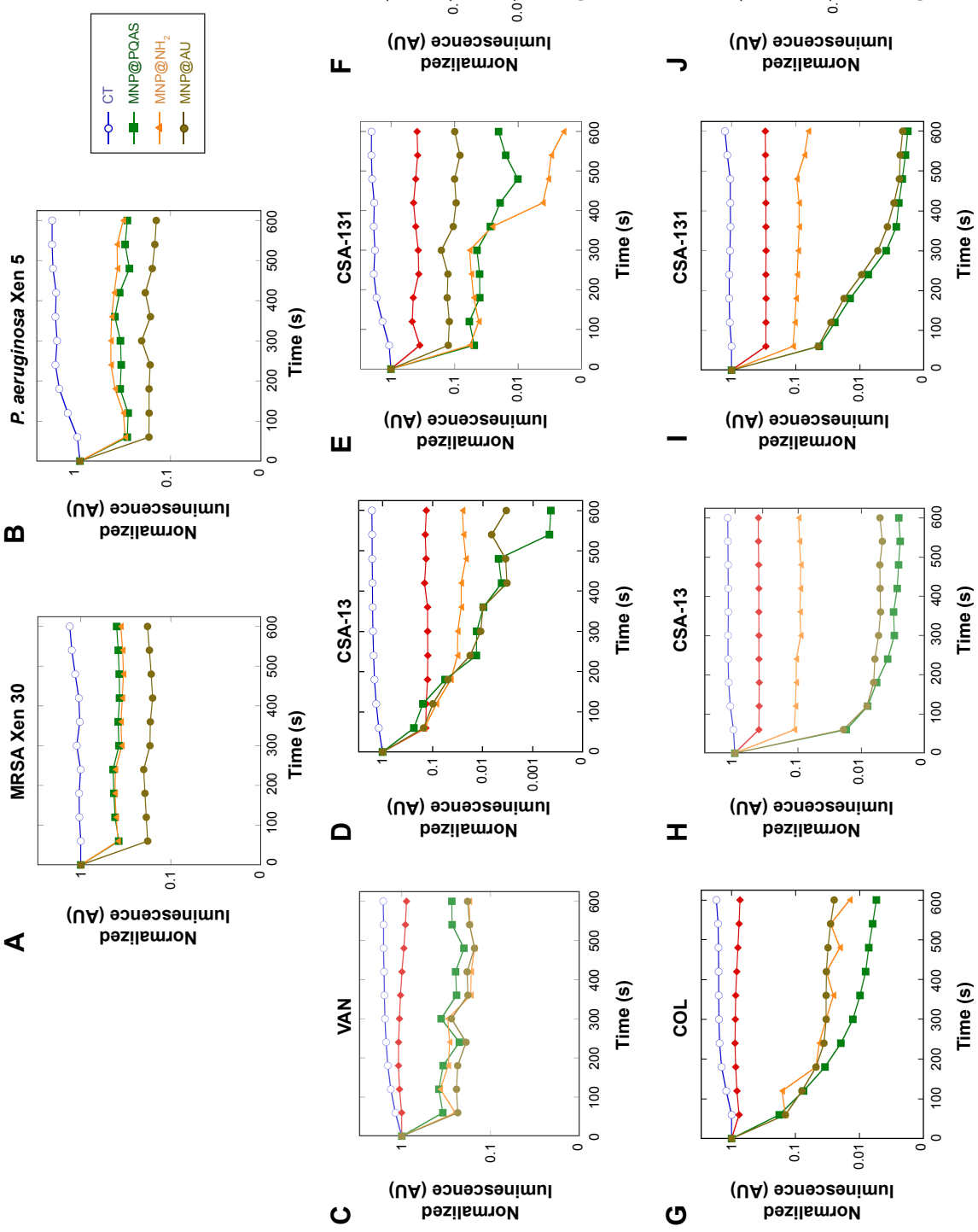

Figure 2 Bactericidal activity of core–shell MNPs in combination with antibacterial agents against MRSA and *Pseudomonas aeruginosa* strains.

Notes: (**A** and **B**) Activity of core–shell nanoparticles: MNP@NH_2 (orange triangles), MNP@Au (gold circles), and MNP@PQAS (green squares) against MRSA Xen 30 and *P. aeruginosa* Xen 5. Bactericidal activity of tested agents: VAN/COL, CSA-13, CSA-131, and LL-37 alone (red rhombus) or in combination with core–shell nanoparticles: MNP@NH_2 (orange triangle), MNP@Au (gold circles), and MNP@PQAS (green squares) against *S. aureus* MRSA Xen 30 (**C**–**F**) and *P. aeruginosa* Xen 5 (**G**–**J**), in comparison to untreated control (CT; blue empty circles).

Abbreviations: MNP, magnetic nanoparticle; PQAS, poly(quaternary ammonium salts); MRSA, methicillin-resistant *S. aureus*; VAN, vancomycin; COL, colistin; CSA, cationic steroid antibiotic; LL-37, cathelicidine LL-37; s, seconds; *S. aureus*, *Staphylococcus aureus*.

Table 2 FIC index of nanoparticles in combination with antimicrobial agents against *Staphylococcus aureus* Xen 30

Tested antibiotics	FIC index	MRSA Xen 30			Interpretation – 1/2/3
		Combination with			
		1 – MNP@NH_2	2 – MNP@Au	3 – MNP@PQAS	
LL-37	FIC index	1	0.0625	0.5	AD/S/PS
CSA-13	FIC index	1	0.5	1	AD/PS/AD
CSA-131	FIC index	1	1	1	AD/AD/AD
VAN	FIC index	1	1	0.26	AD/AD/S

Notes: FIC values >4 indicate antagonistic effects (AN), values between 4 and 1.01 indicate indifference (I), values between 1 and 0.76 indicate additive effects (AD), and values <0.76–0.5 indicate partial synergy (PS) and <0.5 indicate a synergistic effect (S).
Abbreviations: FIC, fractional inhibitory concentration; MRSA, methicillin-resistant *S. aureus*; MNP, magnetic nanoparticle; PQAS, poly(quaternary ammonium salts); CSA, cationic steroid antibiotic; VAN, vancomycin; LL-37, cathelicidine LL-37.

Table 3 FIC index of nanoparticles in combination with antimicrobial agents against *Pseudomonas aeruginosa* Xen 5

Tested antibiotics	FIC index	*P. aeruginosa* Xen 5			Interpretation – 1/2/3
		Combination with			
		1 – MNP@NH_2	2 – MNP@Au	3 – MNP@PQAS	
LL-37	FIC index	0.5	0.14	2	PS/S/I
CSA-13	FIC index	0.13	0.375	1	S/S/AD
CSA-131	FIC index	0.53	1	1	PS/AD/AD
COL	FIC index	1	1	0.5	AD/AD/PS

Notes: FIC values >4 indicate antagonistic effects (AN), values between 4 and 1.01 indicate indifference (I), values between 1 and 0.76 indicate additive effects (AD), and values <0.76–0.5 indicate partial synergy (PS) and <0.5 indicate a synergistic effect (S).
Abbreviations: FIC, fractional inhibitory concentration; MNP, magnetic nanoparticle; PQAS, poly(quaternary ammonium salts); CSA, cationic steroid antibiotic; COL, colistin; LL-37, cathelicidine LL-37.

Table 4 FBC index of nanoparticles in combination with antimicrobial agents against *Staphylococcus aureus* Xen 30

Tested antibiotics	FBC index	MRSA Xen 30			Interpretation – 1/2/3
		Combination with			
		1 – MNP@NH_2	2 – MNP@Au	3 – MNP@PQAS	
LL-37	FBC index	2	0.0625	0.5	I/S/PS
CSA-13	FBC index	1	0.5	1	AD/PS/AD
CSA-131	FBC index	1	1	1	AD/AD/AD
VAN	FBC index	0.53	1	0.13	PS/AD/S

Notes: FBC values >4 indicate antagonistic effects (AN), values between 4 and 1.01 indicate indifference (I), values between 1 and 0.76 indicate additive effects (AD), and values <0.76–0.5 indicate partial synergy (PS) and <0.5 indicate a synergistic effect (S).
Abbreviations: FBC, fractional bactericidal concentration; MRSA, methicillin-resistant *S. aureus*; MNP, magnetic nanoparticle; PQAS, poly(quaternary ammonium salts); CSA, cationic steroid antibiotic; VAN, vancomycin; LL-37, cathelicidine LL-37.

Table 5 FBC index of nanoparticles in combination with antimicrobial agents against *Pseudomonas aeruginosa* Xen 5

Tested antibiotics	FBC index	*P. aeruginosa* Xen 5			Interpretation – 1/2/3
		Combination with			
		1 – MNP@NH_2	2 – MNP@Au	3 – MNP@PQAS	
LL-37	FBC index	0.5	0.16	1.5	PS/S/I
CSA-13	FBC index	0.27	0.625	0.56	S/PS/PS
CSA-131	FBC index	0.53	0.625	0.56	PS/PS/PS
COL	FBC index	1	1	1	AD/AD/AD

Notes: FBC values >4 indicate antagonistic effects (AN), values between 4 and 1.01 indicate indifference (I), values between 1 and 0.76 indicate additive effects (AD), and values <0.76–0.5 indicate partial synergy (PS) and <0.5 indicate a synergistic effect (S).
Abbreviations: FBC, fractional bactericidal concentration; MNP, magnetic nanoparticle; PQAS, poly(quaternary ammonium salts); CSA, cationic steroid antibiotic; COL, colistin; LL-37, cathelicidine LL-37.

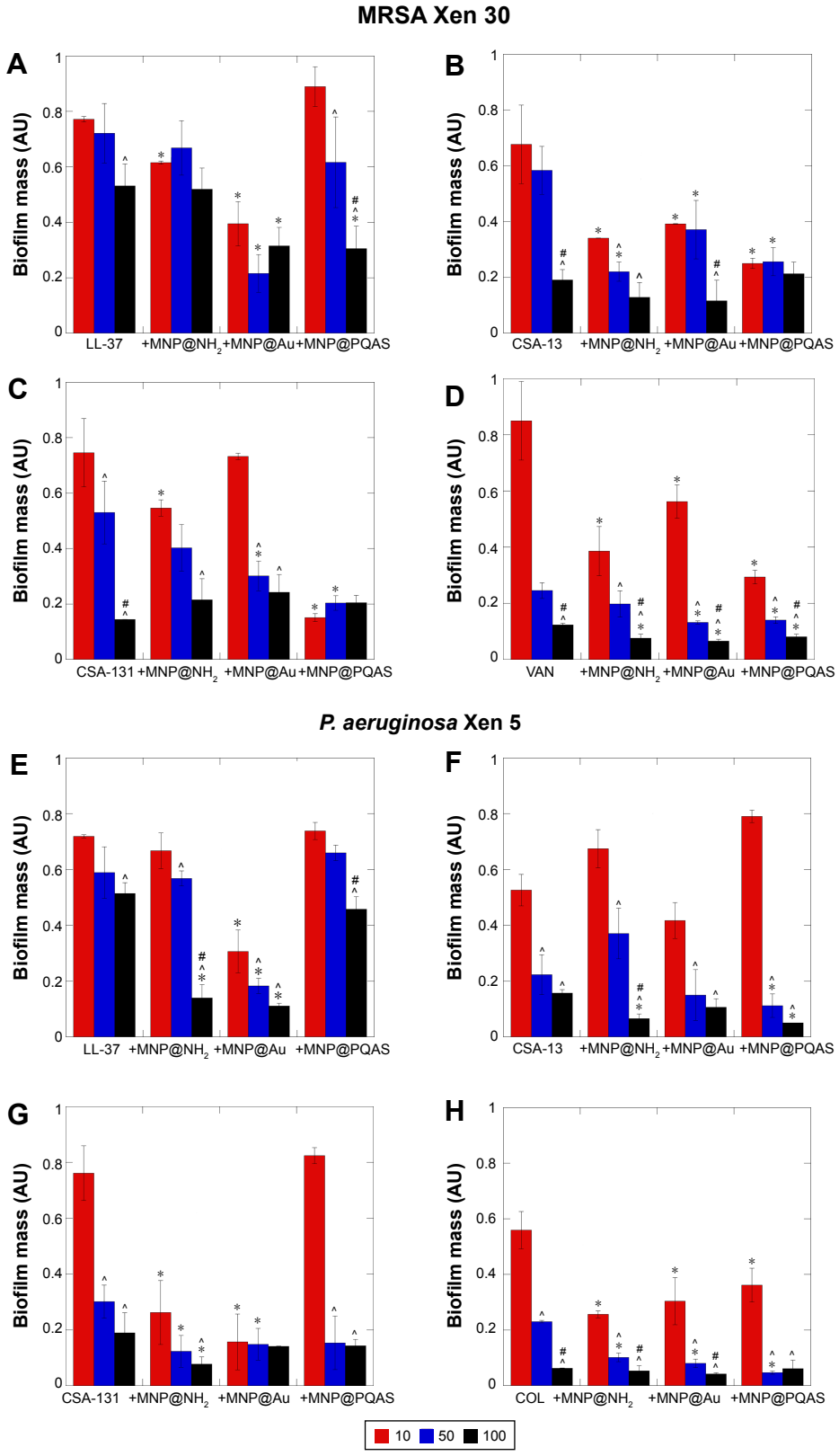

Figure 3 Combination of core–shell MNPs with antibacterial agents strongly restricts formation of biofilm by MRSA and *Pseudomonas aeruginosa* strains.

Notes: Effect of combinatory treatment of core–shell MNPs with membrane-active compounds against MRSA Xen 30 (**A**–**D**) and *P. aeruginosa* Xen 5 (**E**–**H**) when compared to antimicrobial agents alone. In the experiment, agents in doses of 10 μg/mL (red columns), 50 μg/mL (blue columns), and 100 μg/mL (black columns) were used. *Statistical significance ($P<0.05$) compared to antimicrobial agents activity; ^Statistical significance ($P<0.05$) compared to dose 10 μg/mL; #statistical significance ($P<0.05$) compared to dose 50 μg/mL. Results are in response to a one way analysis of variance.

Abbreviations: MNP, magnetic nanoparticle; PQAS, poly(quaternary ammonium salts); MRSA, methicillin-resistant *S. aureus*; LL-37, cathelicidine LL-37; VAN, vancomycin; COL, colistin; CSA, cationic steroid antibiotic; *S. aureus*, *Staphylococcus aureus*; *P. aeruginosa, Pseudomonas aeruginosa*.

Discussion

Cationic antimicrobial peptides (CAPs), such as cathelicidin LL-37, encode an evolutionarily maintained and likely universal mechanism of antimicrobial action against a wide range of pathogens.[36,37] Their mode of action is based on modifications induced in bacterial membrane architecture after CAPs insertion. A higher affinity of CAPs to bacterial cells than host cells is due to the higher negative charge of the bacterial surface driving a semi-specific charge interaction. Different methods have been used to mimic the same molecular properties of CAPs in their synthetic analogs.[38,39]

Ceragenins (CSAs) were developed as a class of bile acid-based derivatives that are cheaper, easier to prepare, purify, and more stable at infection sites due to their resistance to proteolytic degradation than CAPs.[40] Ceragenins possess strong bactericidal activity against Gram-positive and Gram-negative bacteria, including MDR strains.[41–46] Significant membrane activity of CSAs results in bacterial membrane permeabilization and depolarization.[44,47] Previous studies indicate that antimicrobial activity of ceragenins against Gram-negative bacteria is usually lower than the effects against Gram-positive species. The authors suggest that differences in CSA activities are caused by a high content of phosphatidylethanolamine, which might inhibit cationic steroids from binding as well to some bacterial membranes. However, the strong ability of MNPs to significantly decrease the MIC/MBC value for CSAs against Gram-negative bacteria observed in this study suggests that MNPs enhance CSA membrane activity via a synergistic or an additive manner.

Our observations of synergism with MNPs and CSAs are supported by previous observations showing that iron oxide MNPs modulate the interaction of antibiotics from different groups (polypeptides, β-lactams, macrolides, and aminoglycosides) with cellular membrane by increasing the membrane fluidity when antibiotics were fused with nanoparticles.[48] Moreover, Grumezescu et al[49] revealed that MNPs markedly increase amoxicillin activity against representatives of Gram-positive and Gram-negative bacteria. They observed a five- and eightfold reduction of MIC of amoxicillin against *S. aureus* and *Escherichia coli*, respectively.[49] Gu et al[50] indicated that gold nanoparticles strongly enhance VAN activity against VAN-resistant enterococci and observed the ability of this nanosystem to restrict growth of Gram-negative bacteria.

Additionally, results from recent studies indicate that some properties of MNPs, such as resistance to the biodegradation processes, surface activity, and ability to penetrate bacterial cell membranes, are useful for the development of new antibacterial treatments.[51] Recent data show that bare MNPs and their derivatives coated with various functional groups such as carboxyl, isocyanate, and amine decrease the growth of some Gram-positive bacteria strains.[52] The proposed mechanism of antibacterial action of core–shell MNP involves their contribution to interaction with components of pathogen membranes, such as protein F, and restriction of their growth.[17,18] We also observed that nanoparticles interact with bacterial and fungal membranes and are internalized into cells.[18] The proposed mechanism of synergistic action of core–shell nanoparticles with membrane-active agents is summarized in Figure 4.

A notable feature of CSAs, as compared to CAPs, is resistance to protease digestion by enzymes generally present at the site of infection.[53] Additionally, ceragenins, in contrast to CAPs, are resistant to inactivation by DNA or F-actin, which makes them a potential new therapeutic option for cystic fibrosis patients.[54,55]

An important attribute of nosocomial pathogens is the potential to form biofilms on medical devices, which often results in chronic infections.[56] In agreement with published data, our results indicate that biofilm exhibits resistance to low doses of antimicrobial agents.[57] However, the important finding of this study is that application of MNPs as a component of combined therapy significantly reduces the ability of bacteria to form biofilms.

Multiple endogenous antibacterial molecules have been detected in bacterially infected human tissue.[58] This observation suggests that physiologically, antibacterial molecules function in the presence of each other, and their combination may provide a base for synergistic action. Previous published reports related to activity of CAPs at infection sites revealed synergism or additive interactions with other host-secreted antibacterial agents.[59,60] Recent studies confirm that ceragenins also exhibit a synergistic effect with other antibacterial agents such as cefepime and ciprofloxacine.[41,61] Ruden et al[23] revealed that silver nanoparticles act synergistically with polymyxin B. They suggest that silver nanoparticles enhance the intrinsic effect of membrane-active antibiotics.[23]

Combination treatment allows the use of lower doses of drugs compared to monodrug therapy, which enables limited adverse effects of medications. The use of antimicrobial agents with synergy allows also for improving the effectiveness of antibiotics, which may be very beneficial in an era of constantly increasing bacterial resistance to conventional antimicrobial therapy. Additionally, in the case of MDR or

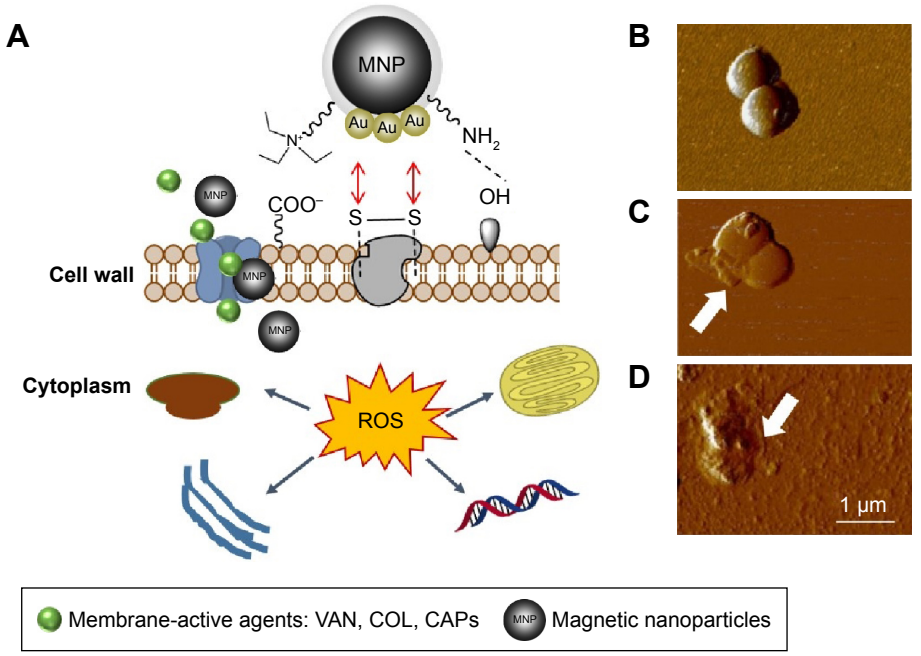

Figure 4 Proposed mechanism of action involving combination of core–shell MNPs with antibacterial agents.
Notes: Core–shell MNPs might interact with compounds of bacteria cell wall and enhance membrane-active agents (VAN, COL, CAPs) insertion and/or uptake. After internalization, MNPs exert oxidative stress causing organelle damage. (**A**) Potential mechanism of action. Atomic force microscopy topography of untreated (**B**), treated with 10 μg/mL CSA-13 (**C**) or 10 μg/mL CSA-13 + MNP@NH_2 (**D**) *Staphylococcus aureus* MRSA Xen 30. Membrane destruction and leakage of the intracellular contents were more pronounced when combined treatment was administrated.
Abbreviations: MNP, magnetic nanoparticle; VAN, vancomycin; COL, colistin; CAPs, cationic antimicrobial peptides; CSA, cationic steroid antibiotic; MRSA, methicillin-resistant *S. aureus*; ROS, reactive oxygen species; *S. aureus*, *Staphylococcus aureus*.

extensively drug-resistant strains, combined therapy has been shown as one way to delay and overcome bacterial resistance.

Combination of nanotechnology with membrane-active compounds, including ceragenins, and classical antibiotics suggests a novel means for the development of new methods to treat and prevent infection caused by MDR pathogens.

Acknowledgments

This work was financially supported by the National Science Centre, Poland, UMO-2012/07/B/NZ6/03504 (to RB) and UMO-2014/15/D/NZ6/02665 (to KN). In 2016 KN was awarded a fellowship from the Foundation for Polish Science (FNP). The equipment used for the analysis in the Center of Synthesis and Analysis BioNanoTechno of University of Bialystok was funded by European Union, as part of the Operational Program Development of Eastern Poland 2007–2013, projects: POPW.01.03.00-20-034/09-00 and POPW.01.03.00-20-004/11. We are grateful to Ms Iwona Misztalewska (TEM) for assistance during data analysis.

Disclosure

The authors report no conflicts of interest in this work.

References

1. Bell BG, Schellevis F, Stobberingh E, Goossens H, Pringle M. A systematic review and meta-analysis of the effects of antibiotic consumption on antibiotic resistance. *BMC Infect Dis*. 2014;14:13.
2. Ozer B, Ozbakıs Akkurt BC, Duran N, Onlen Y, Savas L, Turhanoglu S. Evaluation of nosocomial infections and risk factors in critically ill patients. *Med Sci Monit*. 2011;17(3):H17–H22.
3. Bereket W, Hemalatha K, Getenet B, et al. Update on bacterial nosocomial infections. *Eur Rev Med Pharmacol Sci*. 2012;16(8):1039–1044.
4. Ray GT, Suaya JA, Baxter R. Incidence, microbiology, and patient characteristics of skin and soft-tissue infections in a U.S. population: a retrospective population-based study. *BMC Infect Dis*. 2013;13:252.
5. Watkins RR, David MZ, Salata RA. Current concepts on the virulence mechanisms of meticillin-resistant *Staphylococcus aureus*. *J Med Microbiol*. 2012;61(pt 9):1179–1193.
6. van Belkum A, Melles DC, Nouwen J, et al. Co-evolutionary aspects of human colonisation and infection by *Staphylococcus aureus*. *Infect Genet Evol*. 2009;9(1):32–47.
7. Monecke S, Coombs G, Shore AC, et al. A field guide to pandemic, epidemic and sporadic clones of methicillin-resistant *Staphylococcus aureus*. *PLoS One*. 2011;6(4):e17936.
8. Jones AM, Dodd ME, Morris J, Doherty C, Govan JR, Webb AK. Clinical outcome for cystic fibrosis patients infected with transmissible *Pseudomonas aeruginosa*: an 8-year prospective study. *Chest*. 2010;137(6):1405–1409.
9. Gang RK, Bang RL, Sanyal SC, Mokaddas E, Lari AR. *Pseudomonas aeruginosa* septicaemia in burns. *Burns*. 1999;25(7):611–616.
10. Kluytmans JA, Mouton JW, Ijzerman EP, et al. Nasal carriage of *Staphylococcus aureus* as a major risk factor for wound infections after cardiac surgery. *J Infect Dis*. 1995;171(1):216–219.

11. Mulcahy LR, Isabella VM, Lewis K. *Pseudomonas aeruginosa* biofilms in disease. *Microb Ecol*. 2014;68(1):1–12.
12. Huh AJ, Kwon YJ. "Nanoantibiotics": a new paradigm for treating infectious diseases using nanomaterials in the antibiotics resistant era. *J Control Release*. 2011;156(2):128–145.
13. Niemirowicz K, Markiewicz KH, Wilczewska AZ, Car H. Magnetic nanoparticles as new diagnostic tools in medicine. *Adv Med Sci*. 2012; 57(2):196–207.
14. Wilczewska AZ, Niemirowicz K, Markiewicz KH, Car H. Nanoparticles as drug delivery systems. *Pharmacol Rep*. 2012;64(5):1020–1037.
15. Chomoucka J, Drbohlavova J, Huska D, Adam V, Kizek R, Hubalek J. Magnetic nanoparticles and targeted drug delivering. *Pharmacol Res*. 2010;62(2):144–149.
16. Laurent S, Dutz S, Häfeli UO, Mahmoudi M. Magnetic fluid hyperthermia: focus on superparamagnetic iron oxide nanoparticles. *Adv Colloid Interface Sci*. 2011;166(1–2):8–23.
17. Niemirowicz K, Swiecicka I, Wilczewska AZ, et al. Gold-functionalized magnetic nanoparticles restrict growth of *Pseudomonas aeruginosa*. *Int J Nanomedicine*. 2014;9:2217–2224.
18. Niemirowicz K, Swiecicka I, Wilczewska AZ, et al. Growth arrest and rapid capture of select pathogens following magnetic nanoparticle treatment. *Colloids Surf B Biointerfaces*. 2015;131:29–38.
19. Ghosh IN, Patil SD, Sharma TK, Srivastava SK, Pathania R, Navani NK. Synergistic action of cinnamaldehyde with silver nanoparticles against spore-forming bacteria: a case for judicious use of silver nanoparticles for antibacterial applications. *Int J Nanomedicine*. 2013;8:4721–4731.
20. Brown AN, Smith K, Samuels TA, Lu J, Obare SO, Scott ME. Nanoparticles functionalized with ampicillin destroy multiple-antibiotic-resistant isolates of *Pseudomonas aeruginosa* and *Enterobacter aerogenes* and methicillin-resistant *Staphylococcus aureus*. *Appl Environ Microbiol*. 2012;78(8):2768–2774.
21. Li LH, Yen MY, Ho CC, et al. Non-cytotoxic nanomaterials enhance antimicrobial activities of cefmetazole against multidrug-resistant *Neisseria gonorrhoeae*. *PLoS One*. 2013;8(5):e64794.
22. Jena P, Mohanty S, Mallick R, Jacob B, Sonawane A. Toxicity and antibacterial assessment of chitosan-coated silver nanoparticles on human pathogens and macrophage cells. *Int J Nanomedicine*. 2012;7: 1805–1818.
23. Ruden S, Hilpert K, Berditsch M, Wadhwani P, Ulrich AS. Synergistic interaction between silver nanoparticles and membrane-permeabilizing antimicrobial peptides. *Antimicrob Agents Chemother*. 2009;53(8): 3538–3540.
24. Naqvi SZ, Kiran U, Ali MI, et al. Combined efficacy of biologically synthesized silver nanoparticles and different antibiotics against multidrug-resistant bacteria. *Int J Nanomedicine*. 2013;8: 3187–3195.
25. Rai MK, Deshmukh SD, Ingle AP, Gade AK. Silver nanoparticles: the powerful nanoweapon against multidrug-resistant bacteria. *J Appl Microbiol*. 2012;112(5):841–852.
26. Fayaz AM, Balaji K, Girilal M, Yadav R, Kalaichelvan PT, Venketesan R. Biogenic synthesis of silver nanoparticles and their synergistic effect with antibiotics: a study against gram-positive and gram-negative bacteria. *Nanomedicine*. 2010;6(1):103–109.
27. Gurunathan S, Han JW, Kwon DN, Kim JH. Enhanced antibacterial and anti-biofilm activities of silver nanoparticles against Gram-negative and Gram-positive bacteria. *Nanoscale Res Lett*. 2014;9(1):373.
28. Massart R. Preparation of aqueous magnetic liquids in alkaline and acidic media. *IEEE Trans Magn*. 1981;17(2):1247–1248.
29. Wilczewska A, Markiewicz K. Surface-initiated RAFT/MADIX polymerization on Xanthate-coated iron oxide nanoparticles. *Macromol Chem Phys*. 2014;215(2):190–197.
30. Timurkaynak F, Can F, Azap OK, Demirbilek M, Arslan H, Karaman SO. In vitro activities of non-traditional antimicrobials alone or in combination against multidrug-resistant strains of *Pseudomonas aeruginosa* and *Acinetobacter baumannii* isolated from intensive care units. *Int J Antimicrob Agents*. 2006;27(3):224–228.
31. Kah JCY, Phonthammachai N, Wan RCY, et al. Synthesis of gold nanoshells based on the deposition-precipitation process. *Gold Bull*. 2008; 41(1):23–36.
32. Hussein-Al-Ali SH, El Zowalaty ME, Hussein MZ, Ismail M, Webster TJ. Synthesis, characterization, controlled release, and antibacterial studies of a novel streptomycin chitosan magnetic nanoantibiotic. *Int J Nanomedicine*. 2014;9:549–557.
33. Reddy AJ, Kokila MK, Nagabhushana H, et al. Combustion synthesis, characterization and Raman studies of ZnO nanopowders. *Spectrochim Acta A Mol Biomol Spectrosc*. 2011;81(1):53–58.
34. Kadurugamuwa JL, Sin L, Albert E, et al. Direct continuous method for monitoring biofilm infection in a mouse model. *Infect Immun*. 2003; 71(2):882–890.
35. Wnorowska U, Wątek M, Durnaś B, et al. Extracellular DNA as an essential component and therapeutic target of microbial biofilm. *Stud Med*. 2015;31(2):132–138.
36. Bucki R, Leszczynska K, Namiot A, Sokolowski W. Cathelicidin LL-37: a multitask antimicrobial peptide. *Arch Immunol Ther Exp (Warsz)*. 2010; 58(1):15–25.
37. Zasloff M. Magainins, a class of antimicrobial peptides from Xenopus skin: isolation, characterization of two active forms, and partial cDNA sequence of a precursor. *Proc Natl Acad Sci U S A*. 1987;84(15):5449–5453.
38. Bucki R, Pastore JJ, Randhawa P, Vegners R, Weiner DJ, Janmey PA. Antibacterial activities of rhodamine B-conjugated gelsolin-derived peptides compared to those of the antimicrobial peptides cathelicidin LL37, magainin II, and melittin. *Antimicrob Agents Chemother*. 2004; 48(5):1526–1533.
39. Moore KS, Wehrli S, Roder H, et al. Squalamine: an aminosterol antibiotic from the shark. *Proc Natl Acad Sci U S A*. 1993;90(4):1354–1358.
40. Isogai E, Isogai H, Takahashi K, Okumura K, Savage PB. Ceragenin CSA-13 exhibits antimicrobial activity against cariogenic and periodontopathic bacteria. *Oral Microbiol Immunol*. 2009;24(2):170–172.
41. Bozkurt-Guzel C, Savage PB, Akcali A, Ozbek-Celik B. Potential synergy activity of the novel ceragenin, CSA-13, against carbapenem-resistant *Acinetobacter baumannii* strains isolated from bacteremia patients. *Biomed Res Int*. 2014;2014:710273.
42. Nagant C, Pitts B, Stewart PS, Feng Y, Savage PB, Dehaye JP. Study of the effect of antimicrobial peptide mimic, CSA-13, on an established biofilm formed by *Pseudomonas aeruginosa*. *Microbiologyopen*. 2013; 2(2):318–325.
43. Leszczynska K, Namiot D, Byfield FJ, et al. Antibacterial activity of the human host defence peptide LL-37 and selected synthetic cationic lipids against bacteria associated with oral and upper respiratory tract infections. *J Antimicrob Chemother*. 2013;68(3):610–618.
44. Savage PB, Li C, Taotafa U, Ding B, Guan Q. Antibacterial properties of cationic steroid antibiotics. *FEMS Microbiol Lett*. 2002;217(1):1–7.
45. Chin JN, Rybak MJ, Cheung CM, Savage PB. Antimicrobial activities of ceragenins against clinical isolates of resistant *Staphylococcus aureus*. *Antimicrob Agents Chemother*. 2007;51(4):1268–1273.
46. Chin JN, Jones RN, Sader HS, Savage PB, Rybak MJ. Potential synergy activity of the novel ceragenin, CSA-13, against clinical isolates of *Pseudomonas aeruginosa*, including multidrug-resistant *P. aeruginosa*. *J Antimicrob Chemother*. 2008;61(2):365–370.
47. Lai XZ, Feng Y, Pollard J, et al. Ceragenins: cholic acid-based mimics of antimicrobial peptides. *Acc Chem Res*. 2008;41(10):1233–1240.
48. Istrate CM, Holban AM, Grumezescu AM, et al. Iron oxide nanoparticles modulate the interaction of different antibiotics with cellular membranes. *Rom J Morphol Embryol*. 2014;55(3):849–856.
49. Grumezescu AM, Gestal MC, Holban AM, et al. Biocompatible Fe3O4 increases the efficacy of amoxicillin delivery against Gram-positive and Gram-negative bacteria. *Molecules*. 2014;19(4):5013–5027.
50. Gu H, Ho PL, Tong E, Wang L, Xu B. Presenting vancomycin on nanoparticles to enhance antimicrobial activities. *Nano Lett*. 2003;3(9):1261–1263.
51. Malone ME, Corrigan OI, Kavanagh PV, Gowing C, Donnelly M, D'Arcy DM. Pharmacokinetics of amphotericin B lipid complex in critically ill patients undergoing continuous venovenous haemodiafiltration. *Int J Antimicrob Agents*. 2013;42(4):335–342.

52. Leuba KD, Durmus NG, Taylor EN, Webster TJ. Short communication: carboxylate functionalized superparamagnetic iron oxide nanoparticles (SPION) for the reduction of S. aureus growth post biofilm formation. *Int J Nanomedicine*. 2013;8:731–736.
53. Kuroda K, Fukuda T, Okumura K, et al. Ceragenin CSA-13 induces cell cycle arrest and antiproliferative effects in wild-type and p53 null mutant HCT116 colon cancer cells. *Anticancer Drugs*. 2013;24(8):826–834.
54. Bucki R, Sostarecz AG, Byfield FJ, Savage PB, Janmey PA. Resistance of the antibacterial agent ceragenin CSA-13 to inactivation by DNA or F-actin and its activity in cystic fibrosis sputum. *J Antimicrob Chemother*. 2007;60(3):535–545.
55. Bucki R, Niemirowicz K, Wnorowska U, et al. Polyelectrolyte-mediated increase of biofilm mass formation. *BMC Microbiol*. 2015;15:117.
56. Chatterjee S, Maiti P, Dey R, Kundu A. Biofilms on indwelling urologic devices: microbes and antimicrobial management prospect. *Ann Med Health Sci Res*. 2014;4(1):100–104.
57. Olsen I. Biofilm-specific antibiotic tolerance and resistance. *Eur J Clin Microbiol Infect Dis*. 2015;34(5):877–886.
58. Poletaev A, Boura P. The immune system, natural autoantibodies and general homeostasis in health and disease. *Hippokratia*. 2011; 15(4):295–298.
59. Leszczyńska K, Namiot A, Cruz K, et al. Potential of ceragenin CSA-13 and its mixture with pluronic F-127 as treatment of topical bacterial infections. *J Appl Microbiol*. 2011;110(1):229–238.
60. Singh PK, Tack BF, McCray PB, Welsh MJ. Synergistic and additive killing by antimicrobial factors found in human airway surface liquid. *Am J Physiol Lung Cell Mol Physiol*. 2000;279(5):L799–L805.
61. Bozkurt-Guzel C, Savage PB, Gerceker AA. In vitro activities of the novel ceragenin CSA-13, alone or in combination with colistin, tobramycin, and ciprofloxacin, against *Pseudomonas aeruginosa* strains isolated from cystic fibrosis patients. *Chemotherapy*. 2011;57(6):505–510.